Synthesis and field emission properties of titanium carbide nanowires

Kaifu Huo[1,2], Yemin Hu[1], Yanwen Ma[1], Yinong Lü[3], Zheng Hu[1,4] and Yi Chen[1]

[1] Key Laboratory of Mesoscopic Chemistry of MOE and Jiangsu Provincial Lab for Nanotechnology, School of Chemistry and Chemical Engineering, Nanjing University, Nanjing 210093, People's Republic of China
[2] Hubei Provincial Key Laboratory of Refractories and Ceramics, College of Materials and Metallurgy, Wuhan University of Science and Technology, Wuhan 430081, People's Republic of China
[3] College of Materials Science and Engineering, Nanjing University of Technology, Nanjing 210009, People's Republic of China

E-mail: zhenghu@nju.edu.cn

Abstract
Single crystalline TiC nanowires have been synthesized through a chloride-assisted carbothermal reduction process using active carbon, TiO_2 and NaCl powders as precursors and carbon-coated cobalt or nickel nanoparticles as a catalyst. The products were characterized by x-ray diffraction, electron microscopy, energy-dispersive x-ray spectroscopy and x-ray photoelectron spectroscopy. The TiC nanowires have a face-centred cubic structure with a typical diameter of 20–50 nm and a length of up to a few microns. The formation of the product could be well correlated with the characteristic core–shell structure of the catalyst used. The field emission of the TiC nanowires follows the conventional Fowler–Nordheim behaviour and shows a low turn-on field of about 7.1 V μm^{-1} and good emission stability.

1. Introduction

The study of vacuum electron field emitters has attracted much attention due to their potential applications as field emission (FE) flat-panel displays, microwave power amplifiers, travelling wave tubes, and vacuum microelectronic devices [1–3]. In general, the requirements for field emitters are low turn-on and threshold electric field, high current density, good emission stability as well as high mechanical strength and good thermal and electrical conductivity. To achieve a low turn-on or threshold electric field, the emitters should possess a low work function (ϕ), or a high field enhancement factor (β), or both [4]. One-dimensional (1D) nanostructures such as nanotubes and nanowires are considered to be of ideal geometry for FE because of their sharp tips and high aspect ratio [3], i.e. high β value [2]. Therefore, in recent years, FE properties have been extensively explored in various 1D nanostructures, e.g. in nanotubes of C [5–7], Si [8], AlN [9] and MnO [10], and nanowires or nanorods of Si [11], Mo [12],

W [13], SiC [14, 15], W_2C [16], GaN [17, 18], AlN [19, 20], ZnO [21, 22], CuO [23], Cu_2S [24], NbS_2 [25] and SiCN [26].

Titanium carbide (TiC) is a high temperature ceramic material with a high melting point (3067 °C), high hardness, high thermal and electrical conductivity and high resistance to oxidation and corrosion, which is widely used for cutting tools, wear-resistant coatings and reinforcing components in composites [27, 28]. Along with these good properties, TiC has a relatively low ϕ of about 3.6–4.1 eV [29–32], which is beneficial to FE. In fact, it was previously investigated as an environmentally tolerant field emitter for microelectronic devices [33–35]. It is expected that 1D TiC nanostructures will possess improved FE performance due to the combination of good intrinsic properties of TiC with high β factor. However, little has been done with this topic to date although there are several reports on the preparation of 1D TiC nanowires and nanorods [36–39]. In this paper, TiC nanowires have been synthesized via a chloride-assisted carbothermal reduction route and their FE properties have, for the first time, been examined. The low turn-on field and good emission stability indicate that TiC nanowire is a new promising FE material.

---

[4] Author to whom any correspondence should be addressed.
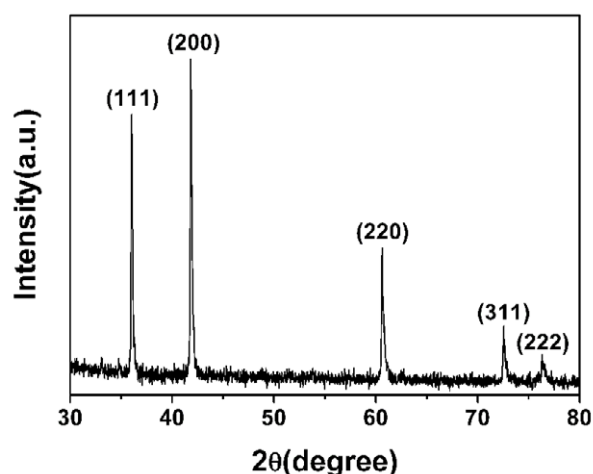
Figure 1. XRD pattern of the as-synthesized TiC product with the Miller indices above the corresponding peaks.

2. Experiments

The carbon-coated cobalt (Co@C) and carbon-coated nickel (Ni@C) nanoparticles with sizes of about 20–50 nm and outer carbon shell thicknesses of about 3–5 nm were provided by Shenzhen Junye Nano Material Co., Ltd (Shenzhen, China). Active carbon and analytical-grade purity reagents of TiO_2 and NaCl powders were purchased from Shanghai Chemical Reagent Company (Shanghai, China). TiC nanowires were synthesized using the following procedure. The well mixed TiO_2, active carbon, NaCl, and Co@C/Ni@C nanoparticles were placed in an alumina boat inside a horizontal tubular furnace. The furnace chamber was evacuated and back filled with pure argon several times to remove oxygen and moisture, and then heated to 1300 °C in pure argon and maintained at this temperature for 60 min. After reaction, the furnace was cooled down to 550 °C in argon and maintained at this temperature for 30 min in air to remove the remaining active carbon.

Scanning electron microscopy (SEM, LEO1530VP, 20 kV), transmission electron microscopy (TEM, JEOL-JEM-1005, 100 kV), high-resolution transmission electron microscopy (HRTEM, JEOL-JEM-2010, 200 kV), energy-dispersive x-ray spectroscopy (EDX, Noran Vantage DS) with HRTEM, as well as x-ray diffraction (XRD, Philips X'Pert Pro) and x-ray photoelectron spectroscopy (XPS, ESCALB MK-II) were used to characterize the product. FE measurements were carried out using a parallel-plate diode configuration in a test chamber maintained at 1.5×10^{-6} Torr. The as-prepared TiC nanowires were screen printed onto a stainless steel plate acting as the cathode. Another plate-shaped stainless steel electrode was used as an anode. High voltage was supplied by a power source (Keithley 248), and the emission current under increasing applied voltage with a step of 100 V was measured using a Keithley 6514 electrometer with an accuracy of 10^{-11} A.

3. Results and discussion

Figure 1 shows the XRD pattern of the as-synthesized product. All of the main diffraction peaks can be indexed to face-centred
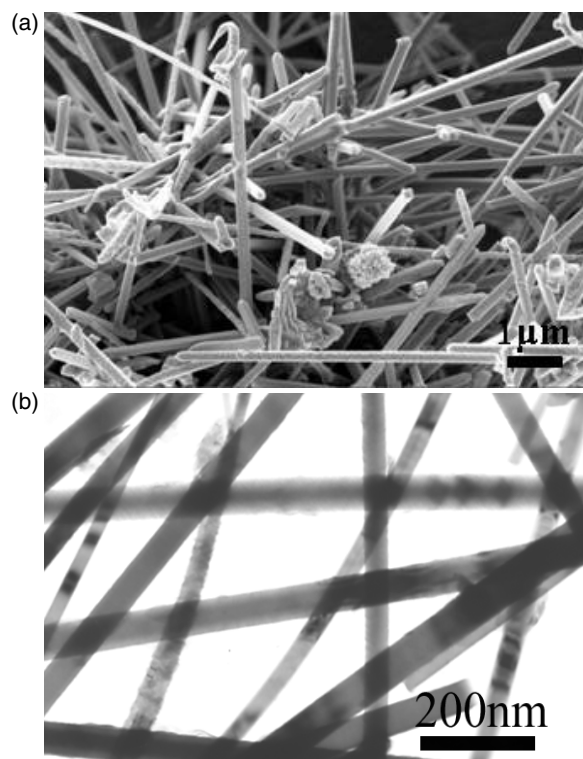

Figure 2. (a) SEM image of the as-prepared TiC nanowires with typical lengths around 10 μm. (b) TEM image of the as-prepared nanowires.

cubic TiC phase (c-TiC, JCPDS card, No. 32-1383), indicating that the product is c-TiC. There are no TiO_2 diffraction peaks in the XRD pattern, suggesting that TiO_2 in the reaction sources is fully converted into TiC in our experiment. The lattice parameter (a) of the as-synthesized TiC product is 0.4318 nm, a little lower than that of the standard value of 0.4327 nm, which indicates that the composition of the as-synthesized TiC product is substoichiometric and the content of Ti atoms is slightly higher than that of C atoms [40]. The SEM image (figure 2(a)) reveals that the TiC product is mainly composed of nanowires with typical lengths of around 10 μm and the corresponding TEM image (figure 2(b)) indicates that the diameter of the nanowires is about 20–50 nm, which is comparable to the size of Co@C or Ni@C catalyst nanoparticles.

Figure 3(a) shows a typical HRTEM image of a TiC nanowire, which provides further insight into the microstructure of the product. The spacing between neighbouring fringes is 0.216 nm, corresponding to the spacing d_{100} of c-TiC. The EDX spectrum of the nanowire (figure 3(b)) exhibits well-resolved strong signals of carbon and titanium as expected. The Cu peaks are derived from the copper grid supporting the specimen. The weak O peak probably comes from the surface amorphous oxide coating of the nanowire as observed in figure 3(a), which was likely formed during the sample transfer and TEM sample preparation. The formation of titanium carbide nanowires was further confirmed through XPS characterization with a non-monochromatized Mg Kα x-ray as the excitation source. High-resolution Ti signals (figure 4(a)) with binding energies of 454.8 and 460.8 eV
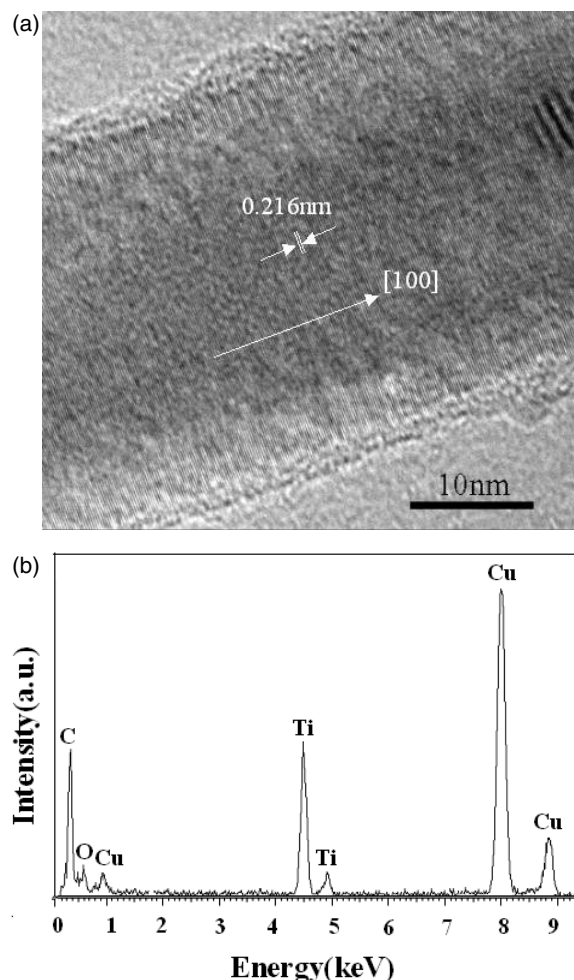
Figure 3. (a) HRTEM image of a typical individual nanowire. (b) Corresponding EDX spectrum of the nanowire.

Figure 4. High-resolution XPS spectra of the as-synthesized TiC nanowires: Ti 2p (a) and C 1s (b) region.

are attributed to the Ti $2p_{3/2}$ and Ti $2p_{1/2}$ peaks of the TiC phase [41], respectively. The C 1s binding energy at 281.4 eV (figure 4(b)) is assigned to the carbon peak in a metal carbide environment [42]. Quantification of the peaks revealed that the TiC nanowire is substoichiometric with the atom ratio of Ti to C of 1.12:1, in agreement with the XRD result. From figure 4(a), it is also noted that, in addition to the main peak around 454.8 eV for Ti $2p_{3/2}$ of Ti–C, there is a satellite peak at the higher binding energy side around 457 eV which is in agreement with Ti $2p_{3/2}$ of Ti–O [43]. This should come from the amorphous oxide coating, consistent with the HRTEM and EDX results (figures 3(a) and (b)).

The above experimental results and analysis show that single crystalline TiC nanowires were prepared in our experiment using active carbon, TiO$_2$ and NaCl powders as precursors and Co@C or Ni@C nanoparticles as a catalyst. The formation mechanism of the TiC nanowires is similar to that of the TiC whiskers which were assigned to the chloride-assisted carbothermal reduction reaction and discussed in detail elsewhere [44]. The main difference between the syntheses of our TiC nanowires and the whiskers in the literature is that we used the core–shell Co@C or Ni@C nanoparticle catalyst here instead of the Co or Ni particles
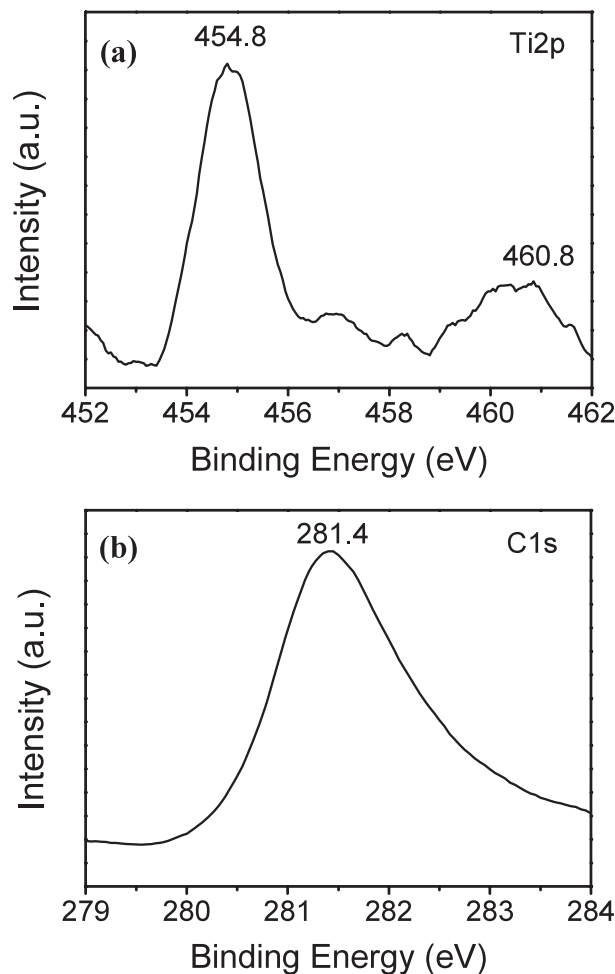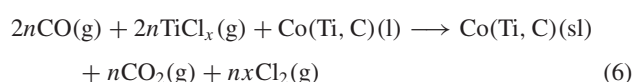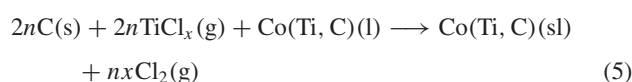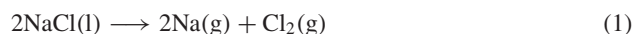
there. Using Co@C/Ni@C nanoparticles gives two main advantages for the formation of TiC nanowires. Firstly, the outer carbon shell of the Co@C/Ni@C nanoparticles effectively prevents the coalescence of Co or Ni nanoparticles in the heating process, which makes the Co/Ni catalyst remain in the nanoscale at the initial stage of TiC nanowire growth. Secondly, the outer carbon shell itself provides the essential C species for nucleation and early growth of TiC nanowires at the reaction temperature. Taking into account this difference, the formation of the TiC nanowires can be understood as follows in the case of Co@C nanoparticle catalysts.
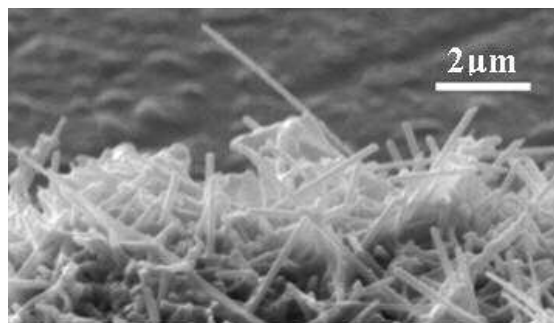
$$2\mathrm{NaCl(l)} \longrightarrow 2\mathrm{Na(g)} + \mathrm{Cl_2(g)} \qquad (1)$$

$$\mathrm{Co@C(s)} \longrightarrow \mathrm{Co(C)(l)} \qquad (2)$$

$$2\mathrm{TiO_2(s)} + x\mathrm{Cl_2(g)} + 4\mathrm{C(s)} \longrightarrow 2\mathrm{TiCl}_x(\mathrm{g}) + 4\mathrm{CO(g)} \qquad (3)$$

$$2\mathrm{TiCl}_x(\mathrm{g}) + 2\mathrm{Co(C)(l)} \longrightarrow 2\mathrm{Co(Ti,C)(l)} + x\mathrm{Cl_2(g)} \qquad (4)$$

$$2n\mathrm{C(s)} + 2n\mathrm{TiCl}_x(\mathrm{g}) + \mathrm{Co(Ti,C)(l)} \longrightarrow \mathrm{Co(Ti,C)(sl)} + nx\mathrm{Cl_2(g)} \qquad (5)$$

$$2n\mathrm{CO(g)} + 2n\mathrm{TiCl}_x(\mathrm{g}) + \mathrm{Co(Ti,C)(l)} \longrightarrow \mathrm{Co(Ti,C)(sl)} + n\mathrm{CO_2(g)} + nx\mathrm{Cl_2(g)} \qquad (6)$$

$$\mathrm{Co(Ti,C)(sl)} \longrightarrow n\mathrm{TiC(s)} + \mathrm{Co(Ti,C)(l)}. \qquad (7)$$

Figure 5. SEM image of the post-treated screen-printed TiC nanowires as the cathode for field emission measurement with a tilt angle view of 60°.

Figure 6. (a) Field emission current density (J) of TiC nanowires as a function of the applied electric field (E). (b) The corresponding F–N plot of the $\ln(J/E^2)$ versus $1/E$. (c) The field emission current stability of the TiC nanowires over time.

Here s, l and g refer to the solid, liquid and gas state respectively; Co(C)(l), Co(Ti, C)(l) and Co(Ti, C)(sl) refer to the liquid Co–C, Co–Ti–C and supersaturated Co–Ti–C alloy droplet, respectively. When the reaction temperature was increased to 1300 °C in Ar, NaCl decomposed to gaseous Na and Cl_2 (reaction 1) and the outer carbon shell of the Co@C nanoparticle dissolved into the molten Co core to form the liquid Co–C alloy droplet (reaction 2). Then, the gaseous $TiCl_x$ species were generated through the reaction of the Cl_2 with active carbon and TiO_2 (reaction 3) [44], which diffused onto the surface of the Co–C droplet, dissociated and dissolved into the droplet to form the ternary Co–Ti–C alloy droplet (reaction 4). When supersaturation was reached due to the continual supply of Ti and C atoms from the gaseous $TiCl_x$ species and active carbon/CO (reactions 5 and 6), TiC species precipitated in such a manner making the liquid–solid interface energy the least and TiC nanowires were gradually formed (reaction 7) [44]. This growth mechanism is also applicable to the case with Ni@C nanoparticles as the catalyst. It is seen that the Ti precursor is the *in situ* generated gaseous $TiCl_x$ species, whereas the C precursor is the carbon shell of the Co@C/Ni@C nanoparticles and active carbon, which might move to the catalyst droplet by solid diffusion (reaction 5), as well as possible gaseous CO (reaction 6). The tight combination of the outer carbon shell with the inner Co/Ni catalyst is beneficial to the initial dissolution of C species into the catalyst droplet, in favour of the growth of TiC nanowires. Much lower yields of TiC nanowires were obtained in our comparison experiments by replacing Co@C/Ni@C with Co/Ni nanoparticles catalyst. It is worth noting that NaCl is necessary for generating the gaseous $TiCl_x$ species as the Ti source (reactions 1 and 3). In a test without NaCl while keeping the other conditions unchanged, no TiC nanowires could be observed in the product, which is consistent with our proposed growth mechanism.

As mentioned in the introduction, TiC nanowire is a new promising FE material. Here, the FE properties of our TiC nanowires have been examined by screen-printing technology, a low-cost process for mass production of large area field emitters [45]. The TiC nanowire paste consisted of TiC nanowires, ethylcellulose, and terpineol with a TiC nanowire content of about 10% in weight. The detailed process for preparing TiC nanowire paste is similar to that for carbo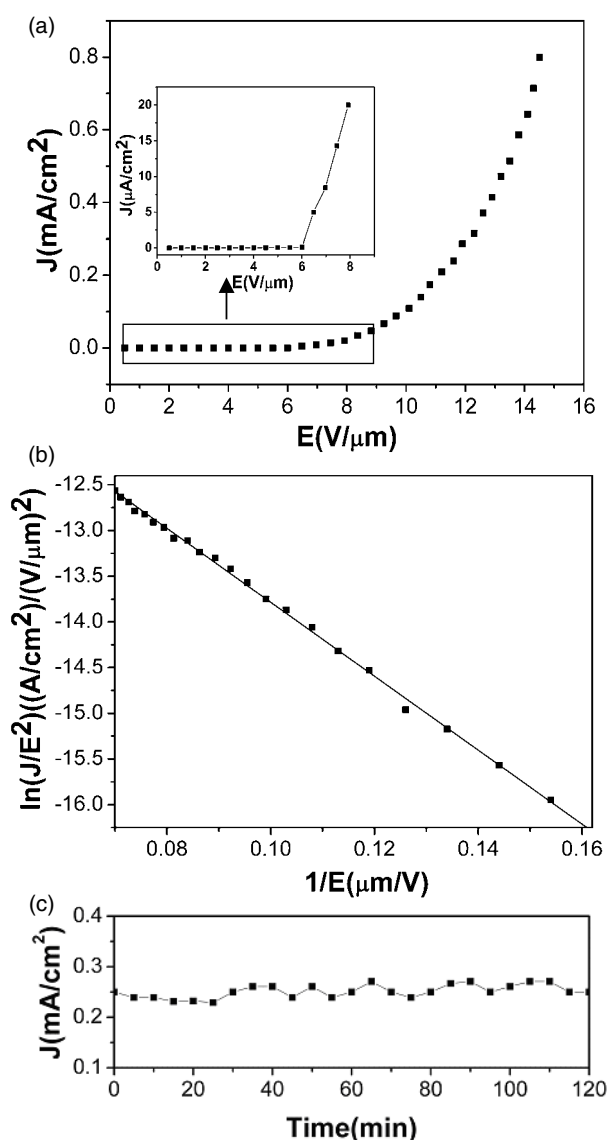n nanotube (CNT) paste described elsewhere [46], and the SEM image of the post-treated TiC nanowires on the cathode with a tilt angle view of 60° is shown in figure 5. A few TiC nanowires protrude from the pasted nanowire film which could contribute more to the overall FE current than other nanowires due to the higher local electrical field. The distance (d) between the cathode of the TiC paste and the stainless steel anode was regulated by a micrometer with an accuracy of 0.001 mm. Its zero value was calibrated by reducing d until electric contact was observed [47, 48].

Figure 6(a) shows the measured field emission current density (J) as a function of the applied electric field (E) with d of 200 μm. J was calculated through dividing the measured emission current by the area of printed TiC nanowire paste, assuming homogeneous electron emission from the sample. It can be seen that the turn-on field (E_{to}), which is usually defined as the electric field to produce a current density of

10 μA cm^{-2} [1], is about 7.1 V μm^{-1}. Above the E_{to}, J increases exponentially with increasing E. When the applied electric field was raised to 14.5 V μm^{-1}, a current density of 0.80 mA cm^{-2} was observed. The E_{to} of TiC nanowires is higher than that of CNTs [1, 45] but superior or comparable to many other 1D field emission materials such as MnO nanotubes [10], SiC nanowires [14], AlN nanorods [20] and nanocones [49], GaN nanorods [50], SiCN nanorods [26], MoO$_3$ nanobelts [51], CuO nanowires [52], SnO nanorods [53] and NiSi$_2$ nanorods [54]. The field emission current–voltage characteristic of the sample was further analysed using the Fowler–Nordheim (F–N) equation [20, 55]:

$$J = (A\beta^2 E^2/\phi)\exp(-B\phi^{3/2}/\beta E)$$

where J is the current density, E is the applied field, ϕ is the work function of the emitting material, β is the field enhancement factor, and A and B are constants with values of 1.56×10^{-10} (A eV V^{-2}) and 6.83×10^3 (V eV$^{-3/2}$ μm^{-1}), respectively. The F–N plot of the ln(J/E^2) versus $1/E$ is shown in figure 6(b). The linearity of the F–N curve within the measurement range confirms that the electron emission from TiC nanowires follows the F–N behaviour. The β value is estimated to be 1174 from the slope of the F–N plot, taking ϕ of TiC as 3.8 eV [29]. The emission stability of the TiC nanowires was examined by measuring the emission with time at a sampling interval of 5 min. Around the current of 200 μA (current density of about 0.25 mA cm^{-2}), no obvious degradation of current density was observed for 2 h continuous operation, as shown in figure 6(c). The current fluctuation was within 10%, showing that the TiC nanowires provide reasonable emission stability, which is important in practical applications.

The post-treatment screen-printed TiC nanowires cathode (figure 5) might have drawbacks such as containing some organic residues, and an insufficient outcrop to the surface or random distribution of the TiC nanowires, similar to the case for a screen-printed CNT paste cathode [56], which could lower the electron emission performance of TiC nanowires. In addition, the amorphous oxide coating on the surface of TiC nanowires may lower the field emission properties of TiC nanowires due to the increase of the potential barrier for electron tunnelling, as is the case for the SiO$_2$-coated taperlike Si nanowires [57]. It is expected that the FE properties could be further improved by patterning the aligned TiC nanowires on a conductive substrate for smaller E_{to}, higher J and better stability.

4. Conclusion

In conclusion, single crystalline TiC nanowires have been synthesized through a chloride-assisted carbothermal reduction with active carbon, TiO$_2$ and NaCl powders as precursors and Co@C or Ni@C nanoparticles as a catalyst. The TiC nanowires possess a face-centred cubic structure with a typical diameter of 20–50 nm and a length of up to microns. The formation of the product could be well correlated with the characteristic core–shell structure of Co@C or Ni@C nanoparticles. The field emission of the TiC nanowires follows the conventional Fowler–Nordheim behaviour and shows a low turn-on field of about 7.1 V μm^{-1} and good emission stability, indicating potential applications.

References

[1] Bonard J M, Kind H, Stöckli T and Nilsson L O 2001 *Solid-State Electron.* **45** 893
[2] Milne W I, Teo K B K, Amaratunga G A J, Legagneux P, Gangloff L, Schnell J P, Semet V, Thien B and Groening O 2004 *J. Mater. Chem.* **14** 933
[3] Xu N S and Ejaz H S 2005 *Mater. Sci. Eng.* R **48** 47
[4] Zhou J, Gong L, Deng S Z, Chen J, She J C, Xu N S, Yang R and Wang Z L 2005 *Appl. Phys. Lett.* **87** 223108
[5] De Heer W A, Chatelain A and Ugarte D 1995 *Science* **270** 1179
[6] De Jonge N and Bonard J M 2004 *Phil. Trans. R. Soc.* A **362** 2239
[7] Fan S S, Chapline M G, Franklin N R, Tombler T W, Cassell A M and Dai H J 1998 *Science* **283** 512
[8] Mu C, Yu Y X, Liao W, Zhao X S, Xu D S, Chen X H and Yu D P 2005 *Appl. Phys. Lett.* **87** 113104
[9] Tondare V N, Balasubramanian C, Shende S V, Joag D S, Godbole V P, Bhorakar S V and Bhadbhade M 2002 *Appl. Phys. Lett.* **80** 4813
[10] Wu M S, Lee J T, Wang Y Y and Wan C C 2004 *J. Phys. Chem.* B **108** 16331
[11] Au F C K, Wong K W, Tang Y H, Zhang Y F, Bello I and Lee S T 1999 *Appl. Phys. Lett.* **75** 1700
[12] Zhou J, Xu N S, Deng S Z, Chen J, She J C and Wang Z L 2003 *Adv. Mater.* **15** 1835
[13] Lee Y H, Choi C H, Jang Y T, Kim E K, Ju B K, Min N K and Ahn J H 2002 *Appl. Phys. Lett.* **81** 745
[14] Zhou X T, Wang N, Au F C K, Lai H L, Peng H Y, Bello I, Lee C S and Lee S T 2000 *Mater. Sci. Eng.* A **286** 119
[15] Lo H C, Das D, Hwang J S, Chen K H, Hsu C H, Chen C F and Chen L C 2003 *Appl. Phys. Lett.* **83** 1420
[16] Wang S J, Chen C H, Chang S C, Uang K M, Juan C P and Cheng H C 2004 *Appl. Phys. Lett.* **85** 2358
[17] Chen C C, Yeh C C, Chen C H, Yu M Y, Liu H L, Wu J J, Chen K H, Chen L C, Peng J Y and Chen Y F 2001 *J. Am. Chem. Soc.* **123** 2791
[18] Ha B, Seo S H, Cho J H, Yoon C S, Yoo J Y, Yi G C, Park C Y and Lee C J 2005 *J. Phys. Chem.* B **109** 11095
[19] Wu Q, Hu Z, Wang X Z, Lu Y N, Huo K F, Deng S Z, Xu N S, Shen B, Zhang R and Chen Y 2003 *J. Mater. Chem.* **13** 2024
[20] Tang Y B, Cong H T, Zhao Z G and Cheng H M 2005 *Appl. Phys. Lett.* **86** 153104
[21] Lee C J, Lee T J, Lyu S C, Zhang Y, Ruh H and Lee H J 2002 *Appl. Phys. Lett.* **81** 3648
[22] Tseng Y K, Huang C J, Cheng H M, Lin I N, Liu K S and Chen I C 2003 *Adv. Funct. Mater.* **13** 811
[23] Zhu Y W, Yu T, Cheong F C, Xu X J, Lim C T, Tan V B C, Thong J T L and Sow C H 2005 *Nanotechnology* **16** 88
[24] Chen J, Deng S Z, Xu N S, Wang S H, Wen X G, Yang S H, Yang C L, Wang J N and Ge W K 2002 *Appl. Phys. Lett.* **80** 3620
[25] Jin Y Z, Hsu W K, Chueh Y L, Chou L J, Zhu Y Q, Brigatti K, Kroto H W and Walton D R M 2004 *Angew. Chem. Int. Edn* **43** 5670
[26] Tarntair F G, Wen C Y, Chen L C, Wu J J, Chen K H, Kuo P F, Chang S W, Chen Y F, Hong W K and Cheng H C 2000 *Appl. Phys. Lett.* **76** 2630
[27] Shin Y S, Li X H S, Wang C M, Coleman J R and Exarhos G J 2004 *Adv. Mater.* **16** 1212

[28] Strzeciwilk D, Wokulski Z and Tracz P 2003 *J. Alloys Compounds* **350** 256

[29] Santerre F, Khakani M A El, Chaker M and Dodelet J P 1999 *Appl. Surf. Sci.* **148** 24

[30] Brauer G, Anwand W, Nicht E M, Coleman P G, Knights A P, Schut H, Kögel G and Wagner N 1995 *J. Phys.: Condens. Matter* **7** 9091

[31] Oshima C, Aono M, Zaima S, Shibata Y and Kawai S 1981 *J. Less-Common Met.* **82** 69

[32] Lindberg P A P and Johansson L I 1988 *Surf. Sci.* **194** 199

[33] Fujii K, Zaima S, Shibata Y, Adachi H and Otani S 1985 *J. Appl. Phys.* **57** 1723

[34] Adachi H, Fujii K, Zaima S, Shibata Y, Oshima C, Otani S and Ishizawa Y 1983 *Appl. Phys. Lett.* **43** 702

[35] Otani S and Ishizawa Y 1991 *Prog. Cryst. Growth Charact.* **23** 153

[36] Wong E W, Maynor B W, Burns L D and Lieber C M 1996 *Chem. Mater.* **8** 2041

[37] Qi S R, Huang X T, Gan Z W, Ding X X and Cheng Y 2000 *J. Cryst. Growth* **219** 485

[38] Wang X J, Lu J, Guo P P and Xie Y 2002 *Chem. Lett.* **8** 820

[39] Liang C H, Meng G W, Chen W, Wang Y W and Zhang L D 2000 *J. Cryst. Growth* **220** 296

[40] Li Y L and Ishigaki T 2003 *Mater. Sci. Eng.* A **345** 301

[41] Ihara H, Kumashiro Y, Itoh A and Maeda K 1973 *Japan. J. Appl. Phys.* **12** 1462

[42] Chang Y H and Chiu H T 2002 *J. Mater. Res.* **17** 2779

[43] Reddy B M, Chowdhury B and Smirniotis P G 2001 *Appl. Catal.* A **211** 19

[44] Ahlén N, Johnsson M and Nygren M 1996 *J. Am. Ceram. Soc.* **79** 2803

[45] Choi W B *et al* 1999 *Appl. Phys. Lett.* **75** 3129

[46] Li J T, Lei W, Zhang X B, Zhou X D, Wang Q L, Zhang Y N and Wang B P 2003 *Appl. Surf. Sci.* **220** 96

[47] Xu X P and Brandes G R 1999 *Appl. Phys. Lett.* **74** 2549

[48] Hu Y M, Huo K F, Chen H, Lu Y N, Xu L, Hu Z and Chen Y 2006 *Mater. Chem. Phys.* **100** 477

[49] Liu C, Hu Z, Wu Q, Wang X Z, Chen Y, Sang H, Zhu J M, Deng S Z and Xu N S 2005 *J. Am. Chem. Soc.* **127** 1318

[50] Kim H M, Kang T W, Chung K S, Hong J P and Choi W B 2002 *Chem. Phys. Lett.* **377** 491

[51] Li Y B, Bando Y, Golberg D and Kurashima K 2002 *Appl. Phys. Lett.* **81** 5048

[52] Hsieh C T, Chen J M, Lin H H and Shih H C 2003 *Appl. Phys. Lett.* **83** 3383

[53] He J H, Wu T H, Hsin C L, Li K M, Chen L J, Chueh Y L, Chou L J and Wang Z L 2006 *Small* **2** 116

[54] Ok Y W, Seong T Y, Choi C J and Tu K N 2006 *Appl. Phys. Lett.* **88** 043106

[55] Gadzuk J W and Plummer E W 1973 *Rev. Mod. Phys.* **45** 487

[56] Kim Y C, Sohn K H, Cho Y M and Yoo E H 2004 *Appl. Phys. Lett.* **84** 5350

[57] Chueh Y L, Chou L J, Cheng S L, He J H, Wu W W and Chen L J 2005 *Appl. Phys. Lett.* **86** 133112